Ceramics International 28 (2002) 819–826

CERAMICS INTERNATIONAL

www.elsevier.com/locate/ceramint

# Role of MgO and $Cr_2O_3$ additives on the properties of zirconia–mullite composites

S. Maitra*, S. Pal, S. Nath, A. Pandey, R. Lodha

*College of Ceramic Technology, 73, Abinash Chandra Banerjee Lane, Kolkata 700010, India*

Received 9 October 2001; received in revised form 21 October 2001; accepted 16 January 2002

## Abstract

Precursor powder for zirconia–mullite composite was synthesized by co-precipitation in aqueous medium taking inorganic salts of aluminium, silicon and zirconium in requisite amounts. The powder was thoroughly characterized in terms of chemical composition, surface area, DTG behavior and FT–IR spectra. Role of two additives, namely, MgO and $Cr_2O_3$, on the densification of the compacted powder at different elevated temperatures ca. 1300–1500 °C was studied by the measurement of different physico-mechanical properties, such as bulk density, apparent porosity, specific gravity, compressive strength, bending strength and fracture toughness. Phase analysis by XRD technique and phase distribution by SEM technique was carried out to evaluate the microstructure of the sintered materials.

*Keywords:* D. Zirconia; D. Mullite; Co-precipitation; Densification; Additives

## 1. Introduction

Several researchers worked on the zirconia–mullite system due to its superior thermo-mechanical properties and different processing routes to prepare $ZrO_2$–mullite composites have been reported. Mizuano et al. [1] prepared $ZrO_2$–mullite composite by sol-gel method using mullite and zirconia sol as the starting materials. The density reached about 100% by firing at 1500 °C. Yoor and Chen [2] produced $ZrO_2$–mullite ceramics from commercial $ZrO_2$ and mullite starting materials, prepared by co-precipitation of TEOS and aluminium nitrate non-hydrate solution. Firing at 1400 °C for 1 h gave fully dense bodies. Shiga et al. [3] used the sol–gel methods to prepare $ZrO_2$ mullite composites. Nearly full density was obtained for the composites containing up to 20 vol.% $ZrO_2$, but that with 25 vol.% $ZrO_2$ showed a slightly lower relative density. Role of different additives on the sintering behaviour and mechanical properties of zirconia–mullite composites were studied by several workers. Orange et al. [4], Leriche [5], and Descamp et al. [6] studied the MgO doped zirconia–mullite composites, which consisted of microstructure with cross-linked mullite grains and inter-granular glassy phase.

In the present work, precursor powder for zirconia–mullite composites was prepared by aqueous phase interaction of the inorganic salts like zirconia oxy chloride, aluminium nitrate and sodium silicate and subsequent gelation of the reaction products from the solution with a proper control of different parameters. The precursor powder was characterized by chemical analysis, measurement of bulk density, surface area, DTGA and FT–IR spectral studies. Two additives, MgO and $Cr_2O_3$, were added to the precursor powder to assess their role on the densification and mechanical properties of the sintered composites. As in the previous works of the author [7], a positive role of $Cr_2O_3$ on the formation of mullite from alumino–silicate precursor was observed. $Cr_2O_3$ was used along with MgO in this work to assess their role on the formation of toughened zirconia–mullite composites from the precursor powder.

## 2. Experimental procedure

For the synthesis of hydrogel $Al(NO_3)_3$, $ZrOCl_2$ of analar quality and liquid sodium silicate (sp. gr. 1.6 and molar ratio of $Na_2O:SiO_2 = 1:3.0$ were selected. Silicic

---

* Corresponding author. Tel.: +91-033-350-1264.
*E-mail address:* maitra_s@vsnl.net (S. Maitra).

0272-8842/02/$22.00
PII: S0272-8842(02)00048-2

acid solution was prepared by following the ion exchange technique. Sodium silicate solution (7% w/v) was passed through a column packed with a Dowex-50 cation exchanger maintaining a flow rate of 200 ml/ min. The silicic acid thus generated through a H-exchanger was stored in a polythene bottle.

Requisite proportions of $ZrOCl_2$, silicic acid and $Al(NO_3)_3$ solution were mixed in a polythene vessel. The solution was clear having a $pH = 2$. Gelation was carried out by slowly adding 1:1 ammonia under stirring whereby viscosity gradually raised and ultimately the mass set to an en block gel at pH 9.5. The gel was processed properly, dried at 60 °C and milled in a pot mill. The powder sample was characterized by chemical analysis, measurement of bulk density, surface area, FT–IR study and DTG analysis.

To the dried powder additives in different proportions were mixed. Sintering of the dried gel powder in compacted form was carried out in an electrically heated muffle furnace at sintering temperatures of 1300, 1350, 1400, 1450, and 1500 °C with a soaking period of 2 h. The sintered mass was characterized by measurement of firing shrinkage, apparent porosity, bulk density and true density. Compressive strength of the sintered 50 mm size cubic samples was measured with a hydraulic compaction-testing machine. The flexural strength of the sintered samples were determined from a three-point bending test with a span of 30 mm and a loading rate of 0.5 mm/min. Fracture toughness was determined by using an indention micro-crack method with a load of 5 kg [8].

X-ray diffraction patterns of the sintered samples were taken with a X-ray diffractometer, using Cu-K$\alpha$ radiation. SEM photographs were taken by S-440 Leo electron microscopy, Cambridge, UK.

## 3. Result and discussion

Solution technique was used in the present investigation to synthesize the precursor powder of the high activity so that superior mechanical properties with uniform microstructure can be achieved. Analar quality reagents were used to avoid any contamination. During mixing very dilute solution of the reactants was used to prevent segregation and agglomeration of the precipitated particles. pH change during precipitation was carefully controlled to avoid sequential precipitation which causes heterogeneity in the mixing and therefore in the precursor powder. High speed stirring was used during precipitation to prevent agglomeration and to break down the agglomerates formed, if any.

To prepare zirconia toughened mullite matrix composite in the present investigation, the mole ratio of the $Al_2O_3:SiO_2:ZrO_2 = 3:2:0.5$ in the precursor powder was intended to keep and from the chemical analysis of the dried hydro-gel (Table 1) it was found that the ratio was more or less maintained in the gel powder. This clearly indicated the complete precipitation of all the cations from the solution and loss of no cation during washing of the gel.

The bulk density of the powder sample was very low, i.e. 0.26 gm/cm$^3$ and the BET surface area was considerably high (240 m$^2$/gm; Table 2) which appears to be significantly high in the inorganic system.

In the FT–IR spectra (Fig. 1) of the powder sample, the absorption band at 3616 cm$^{-1}$ was due to the presence of –OH stretching vibration of the bonded –OH group, –OH bending vibration was observed at 1640 cm$^{-1}$. Si–O stretching vibration was observed at 1020 cm$^{-1}$. Absorption bands at 1385 and 600 cm$^{-1}$ were assigned to Al–O and Zr–O stretching vibrations. So the powder sample contained vibrations of all major bonds, which is an indication that the particle density of the gel powder was low enough to allow the vibration of all the

Table 1
Chemical composition of calcined precursor powder

| Constituents | Batch No. | | | |
|---|---|---|---|---|
| (wt%) | I | II | III | IV |
| $SiO_2$ | 36.29 | 36.23 | 36.13 | 36.06 |
| $Al_2O_3$ | 54.44 | 54.34 | 54.19 | 54.04 |
| $ZrO_2$ | 9.27 | 9.26 | 9.23 | 9.21 |
| MgO | — | — | 0.46 | 0.45 |
| $Cr_2O_3$ | — | 0.18 | — | 0.17 |

Table 2
Physical characteristics of the precursor powder

| Properties | Values |
|---|---|
| Bulk density (gm/cm$^3$) | 0.16 |
| Surface area (m$^2$/gm) | 140 |
| Median particle diameter (μ) | 0.91 |

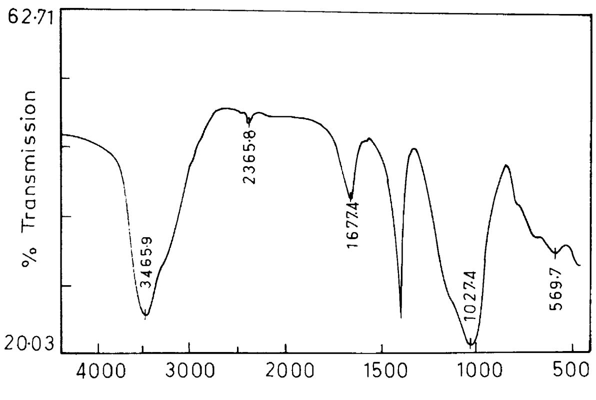

Fig. 1. FT-IR spectra of Batch-I.

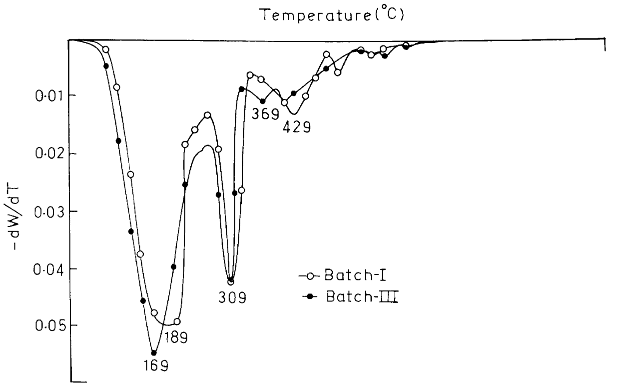

Fig. 2. DTGA diagram of the hydrogels.

major bonds without interference and coupling. It is an evidence of the high surface activity of the gel powder.

From the thermo-gravimetric analysis of the gel materials (Fig. 2), it was observed that the powder gel contained about 35% water. Out of this, about 20% water is lost at about 190–200 °C, about 10% is lost at about 300–310 °C and the rest is lost at about 400–410 °C. By 700 °C, almost all the gel water is eliminated from the sample. The dehydration peaks were assigned to breakage of Zr–OH, Al–OH and Si–OH bonds, respectively, which can be correlated to the ionic potential ($Z^*/r$) value of the cations.

Rager et al. [9] showed that $Cr^{+3}$ can be incorporated in mullite as a replacement of $Al^{+3}$ and this substitution causes lattice expansion in the *c*-axis. Therefore, $Cr_2O_3$ was used as an additive in the present investigation to develop structurally expanded mullite which may create a toughened matrix due to this expansion-induced strain.

MgO was used for the stabilization of zirconia and the proportion of MgO was purposely kept low to produce partially stabilized zirconia with predominantly tetragonal phase in the matrix.

The additives MgO and $Cr_2O_3$ influenced the sintering process of zirconia–mullite composites was evidenced from the volume shrinkage after firing of the materials (Fig. 3). Batch-II which contained $Cr_2O_3$ as an additive showed a regular slight increase in volume shrinkage with the increase in the sintering temperature. $Cr_2O_3$ causes expansion of mullite crystals, as a result of which shrinkage is appreciably off-set with the increase of the sintering temperature. But the batch containing MgO as a sintering aid showed an excessive increase in the shrinkage value at 1450 °C, which might be due to the formation of the liquid phase containing MgO. The decrease in shrinkage value at 1500 °C might be due to the precipitation of MgO at the grain boundary causing pinning of it and thereby restricting the grain movement. This effect is more pronounced in the batch containing both MgO and $Cr_2O_3$ as the sintering additive.

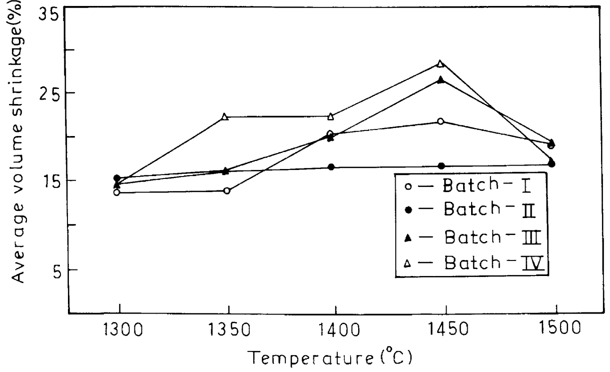

Fig. 3. Average volume shrinkage of the compacts at different sintering temperatures.

Bulk density of the sintered samples more or less increased with the increase in sintering temperature, with some exceptions (Fig. 4). Bulk density depends on the formation of pores and development of different mineralogical phases in the sintered compacts. Maximum bulk density was observed with the batch containing MgO as sintering aid, which is a parallel trend with the volume shrinkage values.

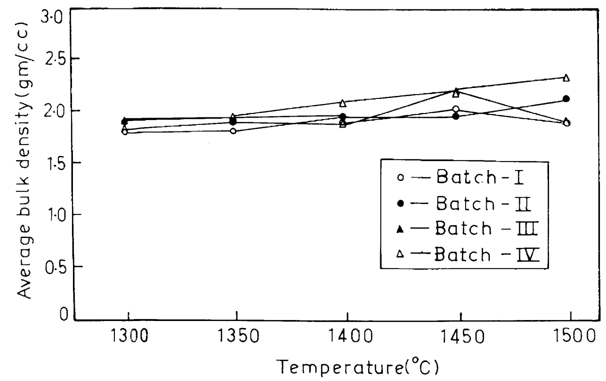

Fig. 4. Average bulk density (gm/cc) of the samples after firing.

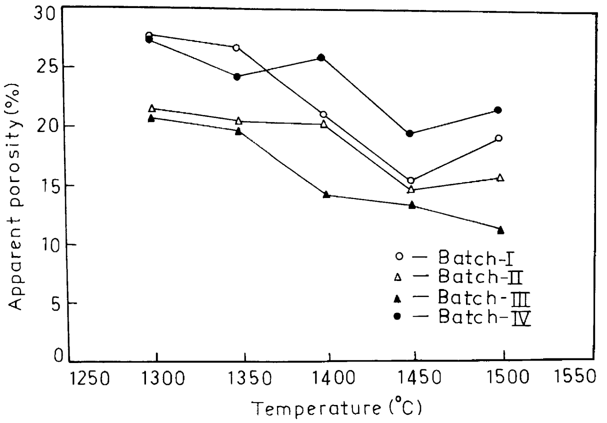

Fig.5. Apparent porosity (%) of the samples after firing.

The apparent porosity values of the sintered samples were also found to be influenced by the additives (Fig. 5). Minimum values of the apparent porosity was observed with the MgO-containing batch. Batches containing both MgO and $Cr_2O_3$ as additives and $Cr_2O_3$ only as additive showed similar trend in the change in apparent porosity values with temperature, though the former contained less apparent porosity. The change in apparent porosity with sintering temperatures may be due to several factors like formation of liquid phase, precipitated phase, secondary crystallization, lattice expansion, micro-crack formation etc.

True density of the sintered samples depends upon the nature and amount of the different phases formed during sintering. Formation of glassy phase in the sintered masses can take place by two ways, (1) due to the presence of trace amount of entrapped salt impurities remained in the gel powder even after repeated washing which may form liquid phase at high temperature, and two, by the complex interaction of the additives in the $ZrO_2$–$Al_2O_3$–$SiO_2$ system with the formation of several eutectics and low melting phases. Maximum value of the specific gravity was observed with the batch containing MgO additives (Fig. 6). Batch containing both MgO and $Cr_2O_3$ also showed a progressive increase in specific gravity value with the increase in the sintering temperature. Batch containing $Cr_2O_3$ as sintering aid did not show much variation in specific gravity with sintering temperature. Though $Cr_2O_3$ can form Cr-substituted expanded mullite lattice, its role on the formation of the crystalline phases further from the amorphous phases is limited. MgO, as a stabilizer of zirconia probably caused precipitation of tetragonal zirconia from $ZrO_2$–MgO solid solution, and also some periclase, which again probably promotes the formation of mullite providing nucleation sites in the microstructure.

The batch containing no additive showed an increase in compressive strength (Fig. 7) at 1350 °C followed by a reduction in compressive strength up to 1450 °C. Beyond this temperature compressive strength further increased. Decrease in compressive is associated with the formation of segregated amorphous phase. Both the batches containing MgO + $Cr_2O_3$ and MgO as additives showed a progressive increase in compressive strength with the sintering temperature, the former showing the maximum increase in compressive strength. Partial stabilization of zirconia by MgO and also blockage of the grain boundary movement by magnesium-containing phases probably resulted in better interlocking of $Cr^{+3}$ containing expanded mullite crystals and reinforcement of mullite matrix by zirconia grains.

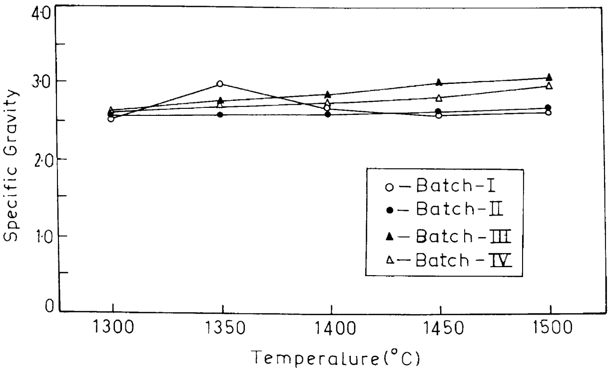

Fig. 6. Specfic gravity of the samples after firing.

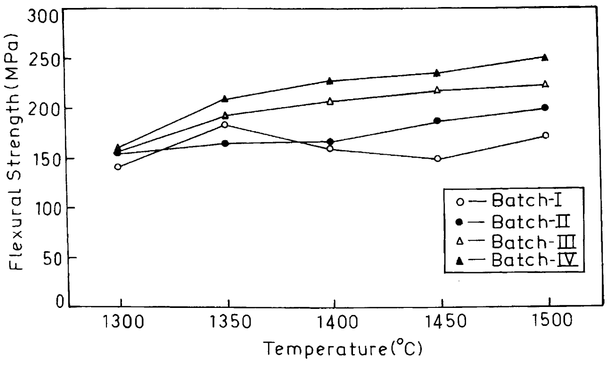

Fig. 8. Flexural strength of the sintered samples after firing (MPa).

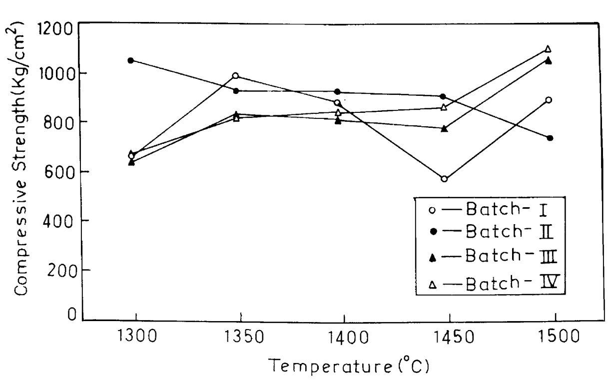

Fig. 7. Compressive strength of the sintered samples after firing in kg/$cm^2$.

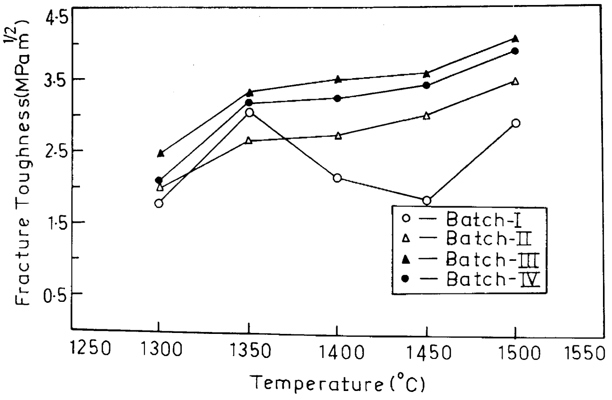

Fig. 9. Change of fracture toughness with increasing sintering temperature.

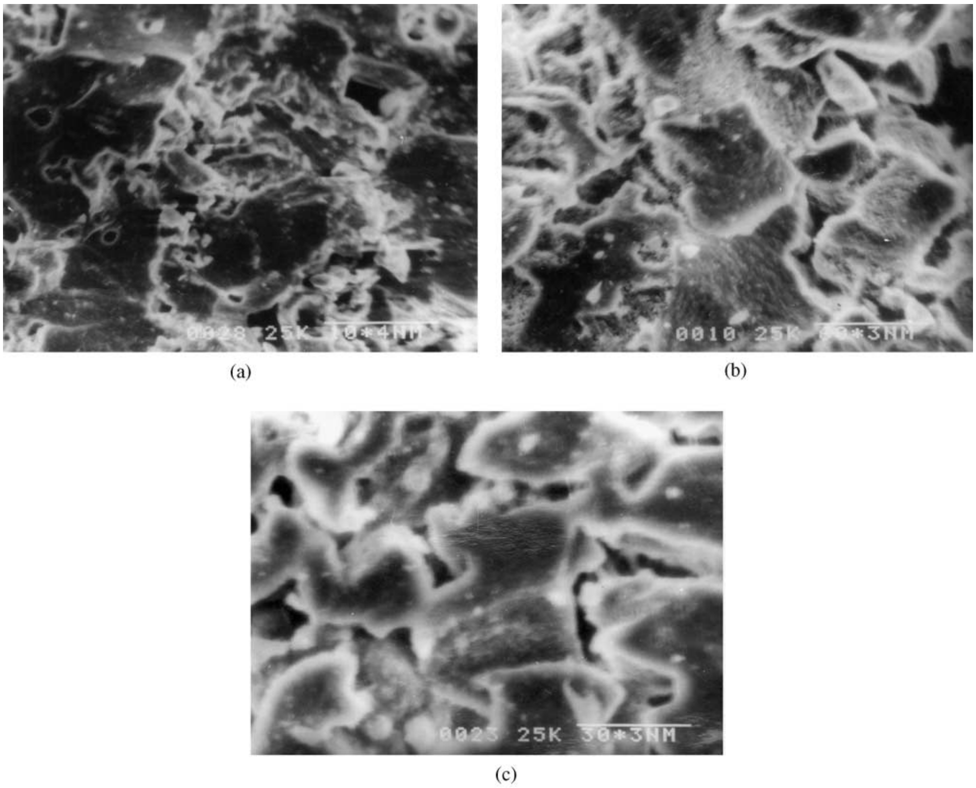

(a) (b)

(c)

Fig. 10. Scanning electron photomicrograph of zirconia–mullite samples (Batch-I).

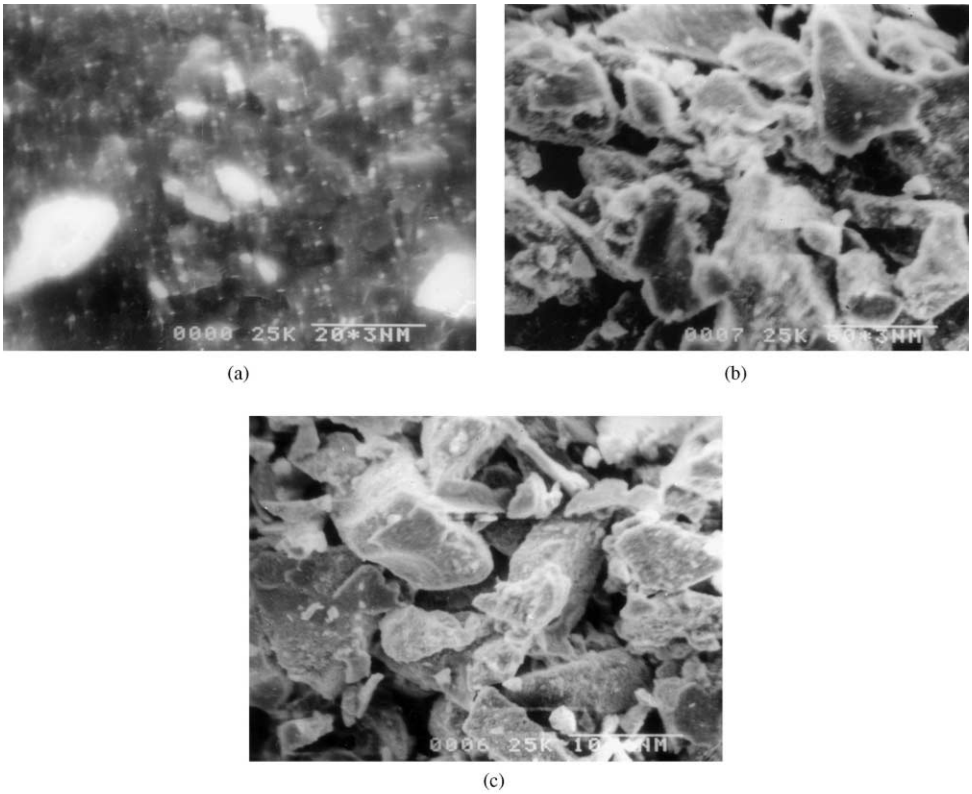

(a) (b)

(c)

Fig. 11. Scanning electron photomicrograph of zirconia–mullite samples (Batch-II).

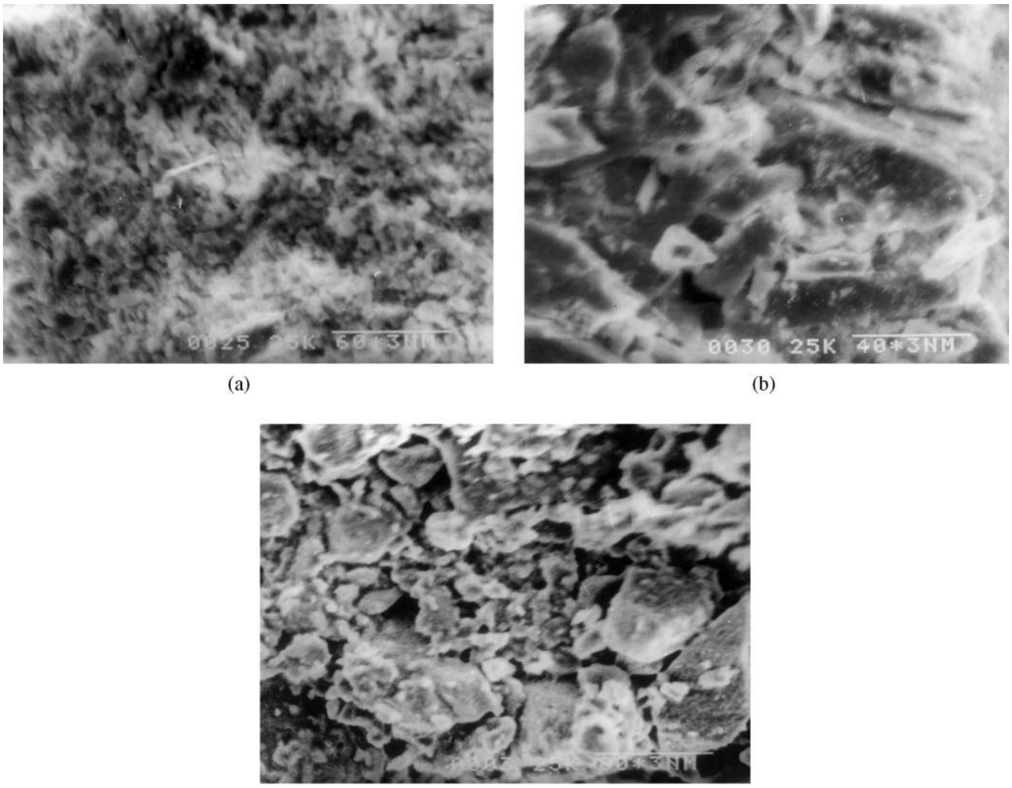

(a) (b)

(c)

Fig. 12. Scanning electron photomicrograph of zirconia–mullite samples (Batch-III).

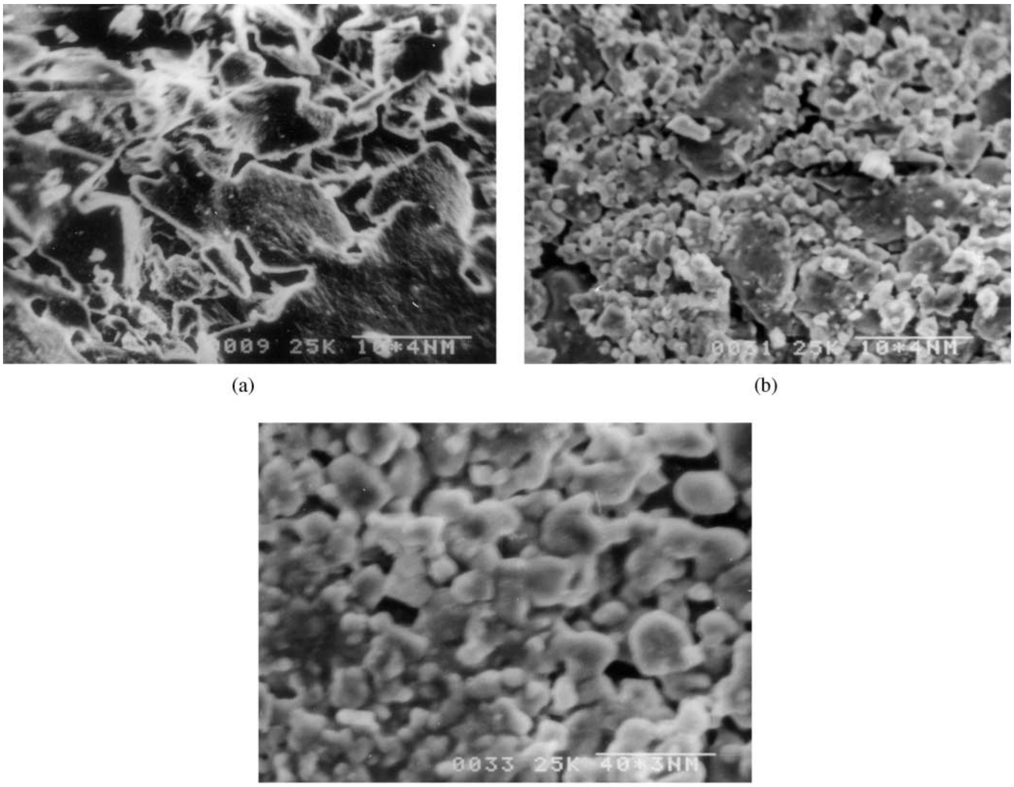

(a) (b)

(c)

Fig. 13. Scanning electron photomicrograph of zirconia–mullite samples (Batch-IV).

The batch containing MgO + $Cr_2O_3$ and MgO showed an increase in flexural strength with the increase in sintering temperature, but the later showed better results (Fig. 8), probably due to the formation of less glassy phase. Batch containing no additive showed the minimum flexural strength. This clearly indicated the positive role of the additives on sintering and formation of better microstructure in this case.

Fracture toughness, $K_{IC}$, of the batches containing MgO + $Cr_2O_3$ and MgO increased with the increase in sintering temperature, and the latter showed better results (Fig. 9). This may be due to a larger amount of transformable $t$-$ZrO_2$ and by a micro-crack nucleation at transformed $m$-$ZrO_2$ particles [10,11].

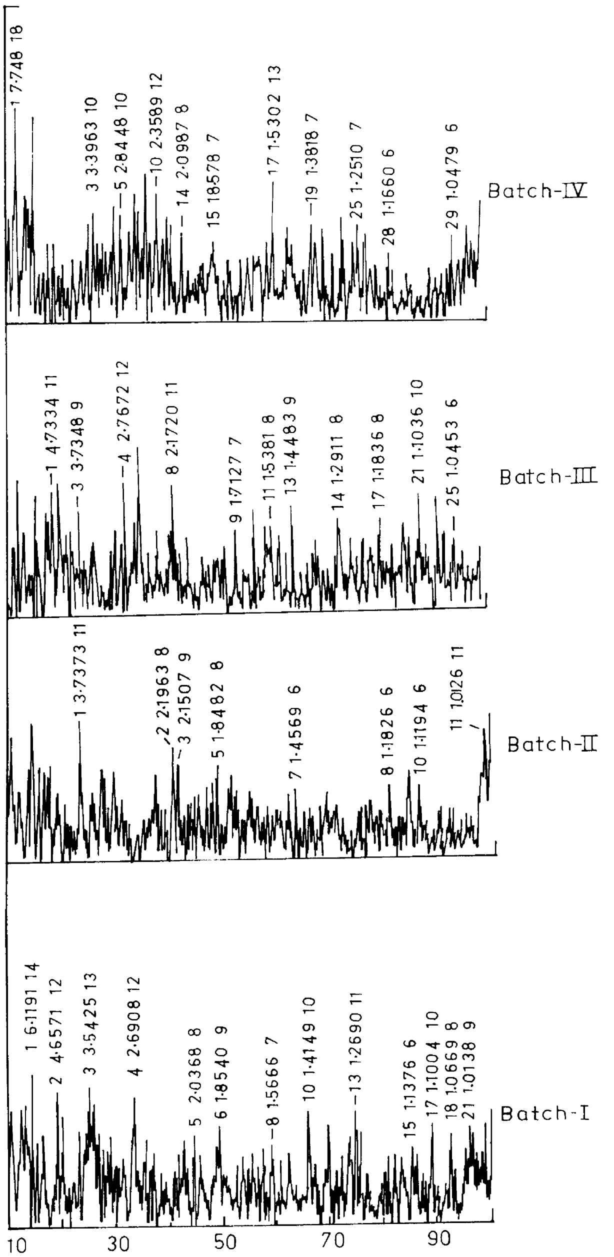

Fig. 14. XRD diagram of zirconia–mullite composites sintered at 1400°C.

From the XRD diagram of the sintered samples (Fig. 10), it was observed that the major crystalline phases are mullite, α-alumina, cristobalite, $t$-zirconia, $m$-zirconia and $c$-zirconia. The proportion of mullite phase was more in the batches containing additives. The proportion of $t$-zirconia was the maximum in the batch containing MgO. In the batch containing MgO + $Cr_2O_3$ minimum amount of cristobalite was observed. Proportion of $c$-zirconia was more in the batch containing MgO + $Cr_2O_3$ and MgO [12].

From the scanning electron micrography of the sintered samples (Figs. 11–14) it was observed that the mullite grains are acicular probably due to a considerable amount of glassy phases present during sintering. The zirconia grains are mainly inter-granular. $ZrO_2$ particles were found to be irregular in size. Mullite/zirconia triple grain junctions had some residual glass, which probably acted as a sink for the impurities in the composites. Rounded morphology of the $ZrO_2$ is due the transient liquid phase, which is also supported by the observation of the glassy phase being invariably associated with $ZrO_2$ grain. Very fine micro-cracks were observed and are revealed in the higher magnification image. High anisotropic volume expansion of $m$-$ZrO_2$ formed from $t$-$ZrO_2$ probably leads to twinning and micro-crack formation at the interfaces depending on crystallography of twins. Sample containing MgO showed better mullite and zirconia grain growth [13,14].

## 4. Conclusion

Inorganic salts can be used to synthesize precursor powders of high surface area and very fine particle size with considerable surface activity by solution technique. MgO and $Cr_2O_3$ as additives play a positive role in the densification and proper microstructure development in the sintered $ZrO_2$–mullite products. The batch containing only MgO as an additive showed a progressive and steady increase in bulk density and specific gravity. The batch containing both MgO and $Cr_2O_3$ as sintering aid contained more glassy phase compared to the batch containing only MgO as a sintering aid. Mechanical properties like compressive strength, flexural strength and fracture toughness of the batch containing both MgO and $Cr_2O_3$ was better than the others. Probably $Cr^{+3}$ doped expanded mullite crystals containing better interlocking matrix with reinforcement from $t$ and $m$-$ZrO_2$, and MgO-containing liquid phase is a reason for this. All the batches contained mullite, corundum, cristobalite, tetragonal, monoclinic and cubic zirconia and some amount of glassy phase. With the incorporation of additives proportion of $t$-$ZrO_2$ increased. Acicular mullite grains with irregular, round shaped, glass-associated zirconia grains were observed in the microstructure. The additives improved the microstructure, in terms of grain growth, phase distribution, strain development etc.

## References

[1] M. Mizuano, M. Shiraishi, H. Saito, Preparation and properties of mullite–ZrO2 composites, in: Abstracts of Annual Meeting of Ceramic Society of Japan, Paper No. 3, F29, Ceramic Society of Japan, Tokyo, 1988.

[2] C.K. Yoor, I.W. Chen, Superplastic flow of mullite zirconia composites, Ceram. Trans. 6 (1990) 567–577.

[3] H. Shiga, M.G.M.U. Ismail, K. Katayama, Sintering of $ZrO_2$ toughened mullite ceramics and its microstructure, J. Ceram. Soc. Jpn 99 (1991) 798–802.

[4] G. Orange, G. Fontozzi, F. Cambier, C. Leblud, M.R. Ansean, A. Leriche, High temperature mechanical properties of reaction sintered mullite/zirconia and mullite/alumina/zirconia composites, J. Mater. Sci. 20 (1985) 2533–2540.

[5] A. Leriche, Mechanical properties and microstructure of mullite zirconia composites, Ceram. Trans. 6 (1990) 541–542.

[6] P. Descamp, S. Sagakuchi, M. Poortemon, F. Cambier, High temparature characteristics of reacton-sintered zirconia–mullite composites, J. Am. Ceram. Soc. 74 (1991) 2476–2481.

[7] N.K. Mitra, S. Maitra, D. Gnanabharathi, T.K. Parya, R. Dey, Effect of $Cr_2O_3$ on the sintering of aluminosilicate precursor leading to mullite formation, Ceram. Int. 27 (2001) 277–282.

[8] B. de la Lastra, C. Leblud, A. Leriche, F. Cambier, M.R. Anseau, $K_{IC}$ calculations for some mullite–$ZrO_2$ composites prepared by reaction sintering, J. Mater. Sci. Lett. 4 (1985) 1099–1101.

[9] H. Rager, H. Schneider, H. Graetsch, Chromium incorporation in mullite, Am. Mineral. 75 (1990) 392–397.

[10] E. Bischoff, M. Ruhle, Thin boundaries in monoclinic $ZrO_2$ particles confined in a mullite matrix, J. Am. Ceram. Soc. 66 (1983) 123–129.

[11] M. Ruhle, N. Claussen, A.H. Heuer, Transformation and microcracking as complementary process in $ZrO_2$-toughened alumina, J. Am. Ceram. Soc. 69 (1986) 195–197.

[12] P.A. Evans, R. Stevens, J.G.P. Binner, Quantitative X-ray diffraction analysis of polymorphic mixes of pure zirconia, Br. Ceram. Trans. J. 83 (1984) 39–43.

[13] S. Prochazka, J.S. Wallace, N. Claussen, Microstructure of sintered mullite-zirconia composites, J. Am. Ceram. Soc. 69 (1986) 66–69.

[14] J.S. Wallace, G. Petzow, N. Claussen, Microstructure and property development of in-situ reacted mullite–$ZrO_2$ composites, Advances in Ceramics 12 (1983) 432–436.